Preparation of High Purity Submicron Powder and Synthesis of Zirconia

Young-Pil Ahn and Bok-Hee Kim

Hanyang University

I. Introduction

Producing methods have been developed to reveal the functions of ceramics for many years.[1-5] Many ceramists have investigated powder preparation, because it was difficult to elevate the properties of ceramics without controlling powders.

The conditions of powders to achieve high performance of ceramics are as follows;

1) Fine particles without agglomeration[6,7]
2) Narrow particle size distribution[8]
3) Sphere-shaped particles[9]
4) Homogeneous composition between particles[10]
5) Hih purity of particles[11]

There are many processes of preparing powders such as spray drying,[12] liquid drying,[13] plasma spraying,[14] vapor phase reaction,[15] freeze drying,[16] coprecipitation,[17] hydrolysis,[18] sol-gel process,[19] but there are also many problems such as long reaction time, complex process, preferential reaction, and special raw materials. At this point, it is not determinative to satisfy the above conditions of ceramic powders. So ceramics have excellent functions compared to metal or organic polymer, but there are many difficulties to apply to the engineering materials realistically.

In the result, microstructure of ceramics must be designed to perform the functions and powders must be controlled to design the microstructure. It is indispensable to determine the process of powder preparation.

In this study for the ZrO_2 ceramics which is applicable to many fields such as mecanical ceramics,[20-26] refractory,[27] electrolyte cells,[28] and sensors. Simple process which was reciprocals of coprecipitation was employed to solve many problems causing in the powder preparation procedure.

That is,

1) Inhibition of preferential reaction according to the pH value (homogeneous composition between particles)
2) Inhibition of agglomeration

3) Inhibition of growth of particle (large surface area)
4) Mass production of powders
5) Simple process

2. Comparison of powders according to the process

2.1 Raw materials

Table 1 shows the raw materials used in this experiment. Each raw materials was dissolved into the distilled water and used.

Table 1. Raw Materials

Raw Materials	Company	Purity	Sol. Concen.
$ZrOCl_2 \cdot 8H_2O$	Kokusan Chem. Works, Ltd.	Chem. Pure	0.2 mol
$Mg(NO_3)_2 \cdot 6H_2O$	Tokyo Chem. Co., Ltd.	Chem. Pure	0.2 mol
$Ca(NO_3)_2 \cdot 4H_2O$	Kokusan Chem. Works, Ltd.	Chem. Pure	0.2 mol
$YCl_3 \cdot 6H_2O$	Fluka AG	99.9 %	0.1 mol
NH_4OH	Shinyo Pure Chemicals	First grade	1.5, 5-N

2.2 Powder preparations

Coprecipitation method and spraying method were used to compare powders according to the methods in the system of (1-x) ZrO.

Coprecipitation method and spraying method were used to compare powders according to the methods in the system of (1-x) ZrO_2 – xMgO (x=0.0, 0.1, 0.3, 0.5). Solutions of raw materials were mixed for 12 hours to prevent separation of solution by the gravity.

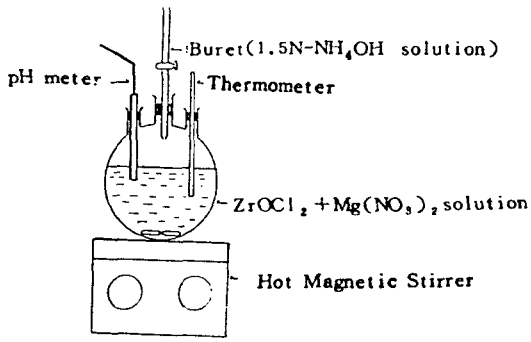

Fig. 1. Schematic view of apparatus for preparing powder by coprecipitation

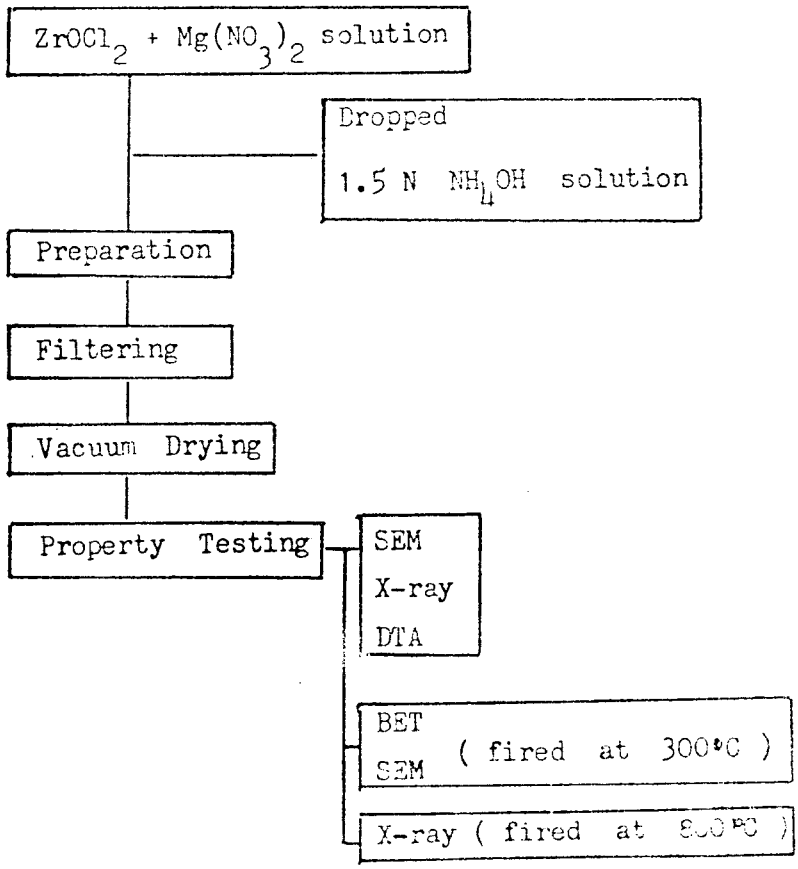

Fig. 2. Flow Chart of Coprecipitative Preparation.

First, 1.5N-NH_4OH was dropped into the mixed solution and coprecipitates were obtained **(Fig.1 and 2)**. Temperature of mixed solution was kept at 40°C constantly. The rate of drop of NH_4OH was 5ml/hr and the mixed solution was stirred by magnetic stirrer. After finishing this reaction, strong NH_4OH was put into the mixed solution to determine the end of reaction.

Second, the mixed solution was sprayed into 5N-NH_4OH solution and the precipitates were obtained **(Fig. 3 and 4)**. Spraying was done through the nozzle of 0.5mm diameter, by the rate of 10 l/min of compressed air. The 5N-NH_4OH was stirred during reaction on the magnetic stirrer. In schematic view of Fig.3, double tube of spray was used to keep the amount of spray constantly and spray droplet finely and uniformly.

The precipitates obtained by these two processes were filtered, washed and dryed in the vacuum dryer. The amount of Cl in powders analyzed by WDX was only trace.

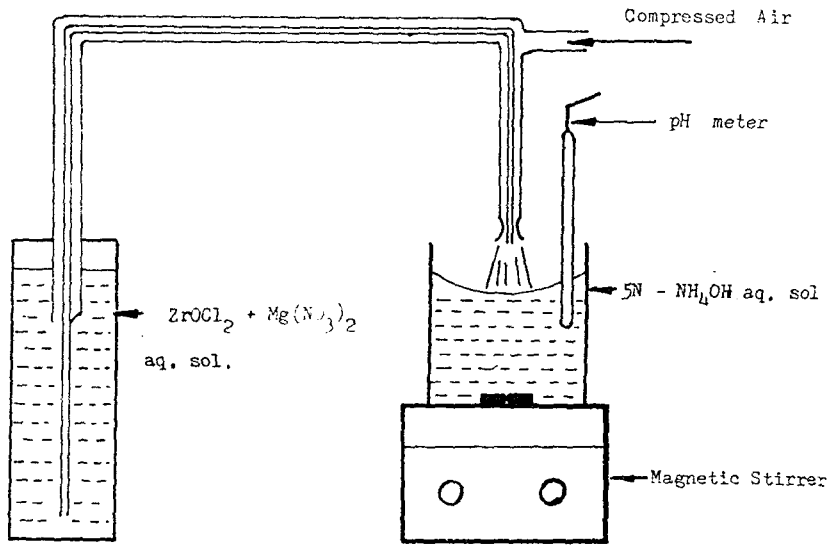

Fig. 3. Schematic view of apparatus for preparing powder by spraying method

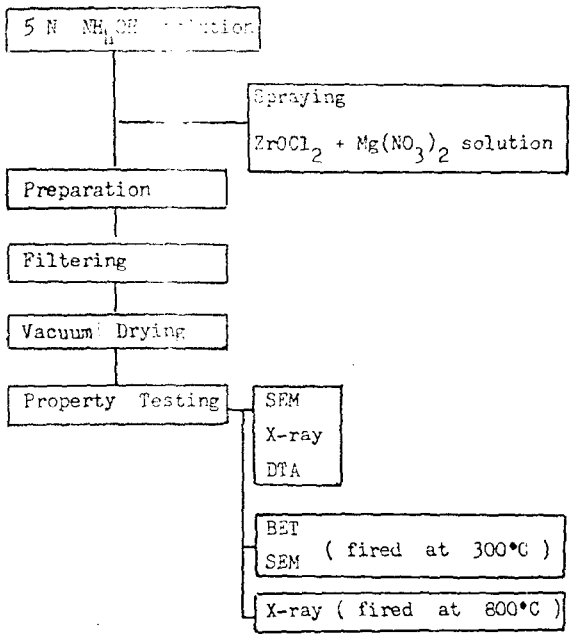

Fig. 4. Flow Chart of Pneumatic Spraying Preparation.

2.3 Results

2.3.1 The change of precipitates with pH variables

Fig. 5 shows the changes of precipitate according to the pH in the (1-x) ZrO_2-xMgO (x=0.5) system. In this figure, precipitate reaction began from strong acid to pH4 and was not changed between pH4-pH8. Precipitate was increased from pH8 and finished at pH10. No change of precipitates between pH4 and pH8 was based on the finish of ZrO $(OH)_2$ precipitates at pH4

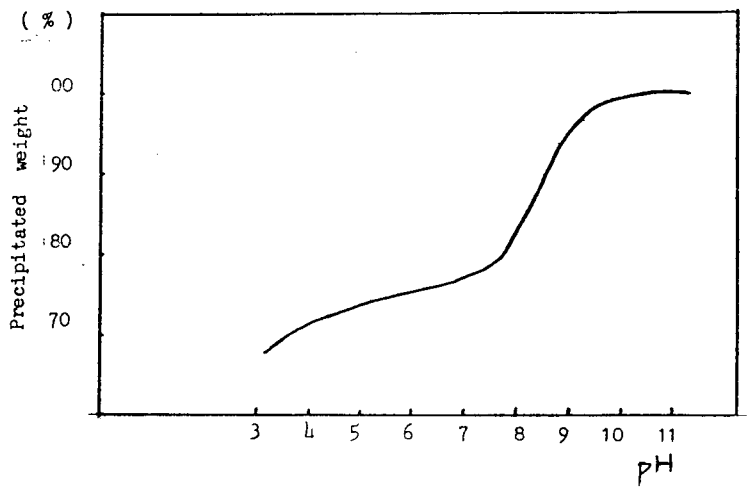

Fig. 5. The change of precipitated weight with pH variable

and increasing of precipitates from pH8 to pH10 was the precipitation of $Mg(OH)_2$. $Mg(OH)_2$ precipitates under pH12 which began to precipitate was inferred from the coexistance of $ZrO(OH)_2$ in the solution.

From this result, precipitate in the spraying method was obtained in 5N-NH_4OH solution because the pH of solution after reaction was above pH10.

2.3.2 Characteristics of Powders

Fig.6 and 7 shows the DTA curves of powders obtained by the coprecipitation and

spraying processes. In this figure, endothermic reactions at 90°C 150°C and exothermic reaction occurred at 400°C The first endothermic at 90°C was vaporization of absorption water and the second at 150°C was decomposition of $ZrO(OH)_2$. Exothermic was due to the crystallization. Endothermic at x=0.5 about 400°C was inferred from decomposition of $Mg(OH)_2$. Crystallization temperature was increased with the amount of MgO.

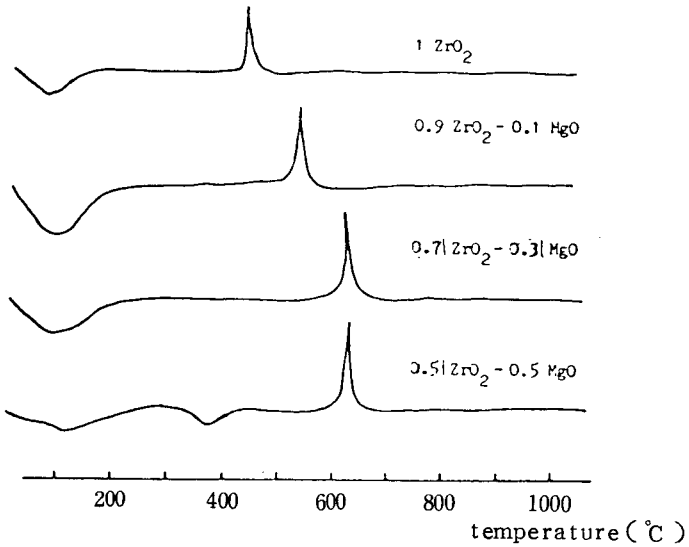

Fig. 6. DTA curves of powders prepared by coprecipitation in $(1-x)ZrO_2$-xMgO system

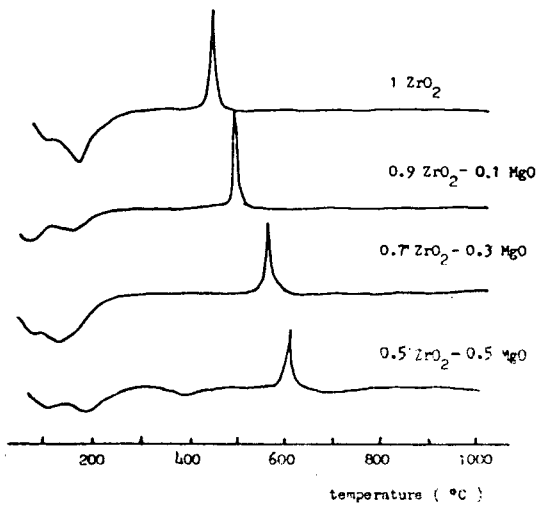

Fig. 7. DTA curves of powders prepared by spraying method in $(1-x)ZrO_2$-xMgO system

X-ray diffraction patterns of powders heat treated at 800°C is shown in **Fig. 8 and 9.** In the X-ray diffraction paterns, difference between coprecipitation and spraying was at x=0.1. Cubic and monoclinic phases were mixed in the powders by coprecipitation at x=0.1 but only cubic phases was in the powder produced by spraying method. Particle growth caused the mixed crystal phase by the long reactiontime. In spray, reaction time was very short and particle growth was inhibited.

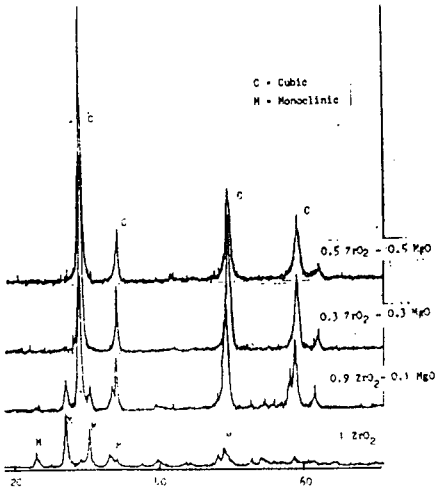

Fig. 8. X-ray diffraction patterns of specimens prepared by coprecipitaton in (1-x) ZrO_2- xMgO system

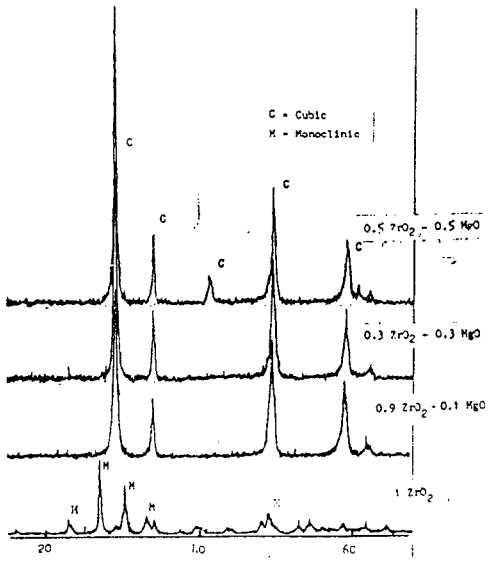

Fig. 9. X-ray diffraction patterns of specimens prepared by spraying spraying method in $(1-x)ZrO_2$-xMgO system

Scanning electronic micrographs of powders obtained by two processes were **Fig.10. Fig.10** (a) shows agglomerated and grown particle. Fig.10(b) shows separated and spherical powders with 1-10μm diameter.

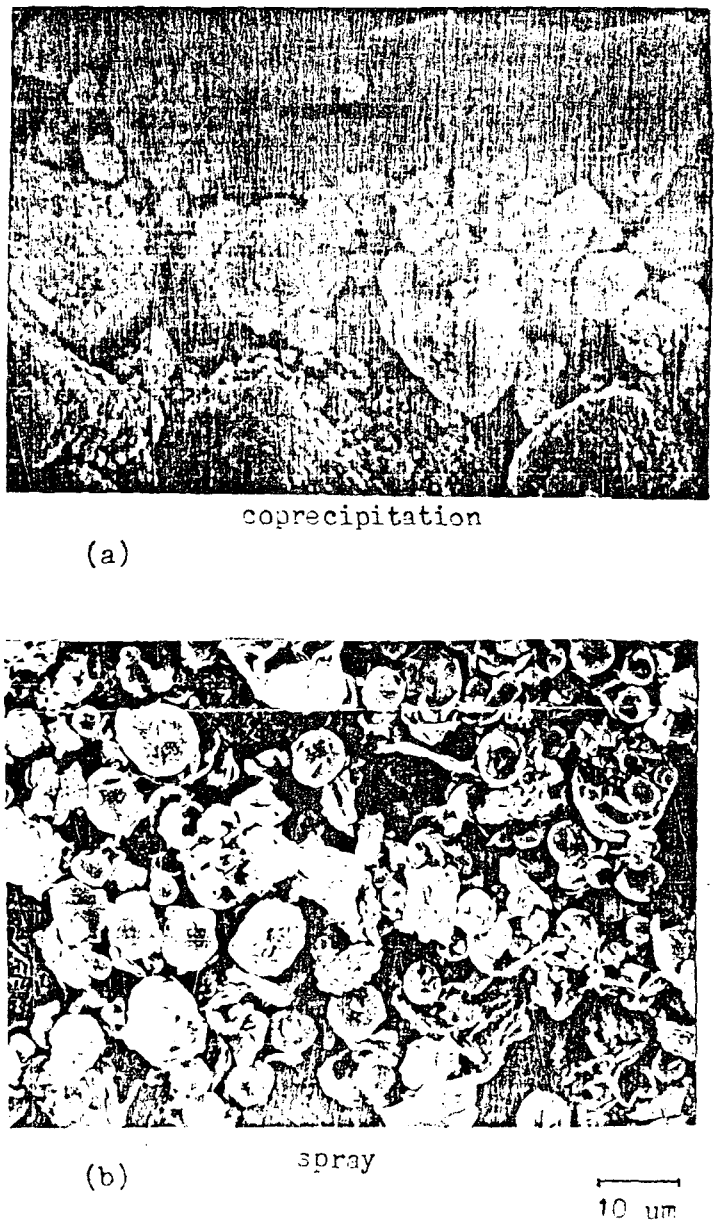

Fig.10. SEM photograps of prepared powder (x=0.1)

Surface area of powders is listed in the **Table 2.** Surface area of spraying method was about 10 times bigger than that of coprecipitation.

Table 2. BET Results of (1-x)ZrO2-xMgO System at 300 C Heating

	Surface Area (m^2/g)	
	Co-precipitate	Spraying
1 ZrO2	10.991	149.341
0.9ZrO2-0.1MgO	13.430	134.179
0.7ZrO2-0.3MgO	20.685	111.124

Fig.11 shows the particle size distribution. Powders obtained by spraying method had narrow distribution range of 1-10μm and fine size.

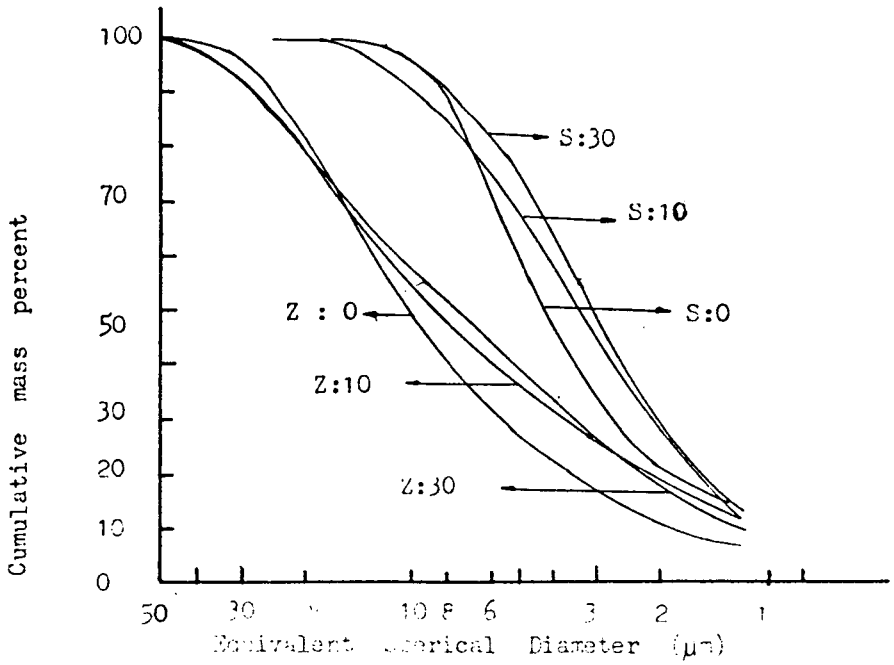

Fig. 11. Particle size distribution

2.4 Discussion of powder preparation method

DTA and X-ray diffraction patterns were not so different but conspicuously different in particle shape, size, size distribution and surface area between coprecipitation and spraying methods.

In coprecipitation, spontaneous reaction at contacted surface between NH_4OH droplet and mixed solution, long time reaction and preferatial reaction with pH variables caused particle growth, agglomeration and heterogeneous composition. But reaction surface in spraying method was so large that spontaneous reaction could be occured in short time overall. Inhibition of agglomeration, spontaneous coprecipitation reaction (homogenization of composition), sphere type, narrow size distribution, large surface area and mass production of powders were achieved by simple spraying method. This method was desirable to produce powders to promote sintering.

3. Powder preparation in the system of ZrO_2-Y2O3 and ZrO_2-CaO

3.1 ZrO_2-Y_2O_3 system

3.1.1 Powder preparation

Raw materials in Table 1 were used to prepare powders in the system of (1-x)ZnO_2-xY_2O_3 (x=0.01, 0.03, 0.06, 0.09). Each solution was mixed in accordance with (1-x) ZrO_2-xY_2O_3 for 12 hours on the magnetic stirrer. Powders in ZrO_2-Y_2O_3 system were produced with apparatus of **Fig.12.** Procedure is **Fig.13.** **Fig.14** shows the DTA curves of powders. Endothermic

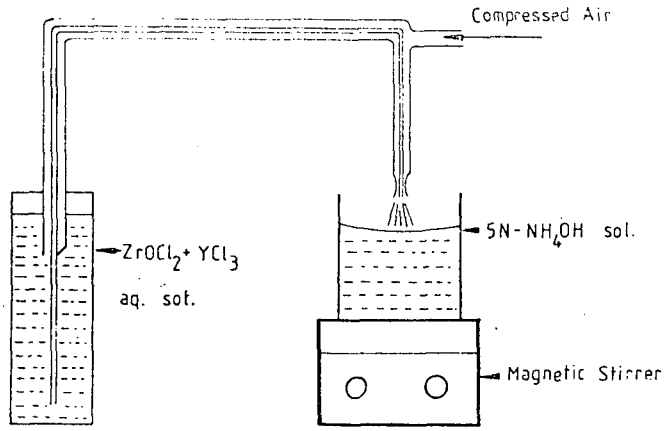

Fig. 12. Schematic view of apparatus for preparing powder by spraying method

reactions between 100-200°C were vaporization of absorption water and decomposition of ZrO $(OH)_2$. Exothermic reactions above 700°C was crystallization of amorphous powder and shifted to the higher temperature with the amount of Y_2O_3. **Fig.15** shows the X-ray diffraction patterns of powder calcined at 900°C for 2hr. Crystal structure was monoclinic in the case of x=0.01. Above x=0.03, crystal structure was cubic phase and stabilized. Particle size of powder is **Fig.16.** Surface area is in **Table 3.** Powders had narrow distribution in the range of 1-10μm and large surface area.

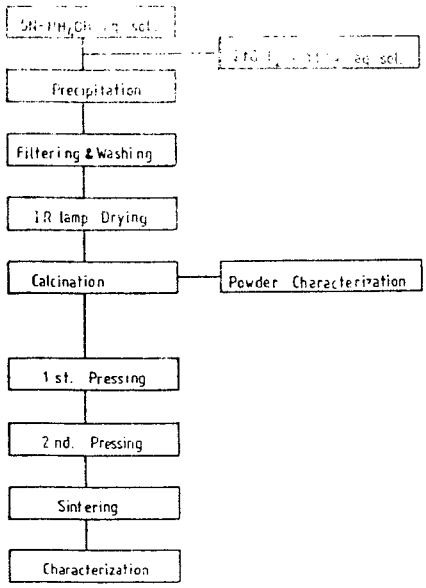

Fig. 13. Flow chart of experimental procedure

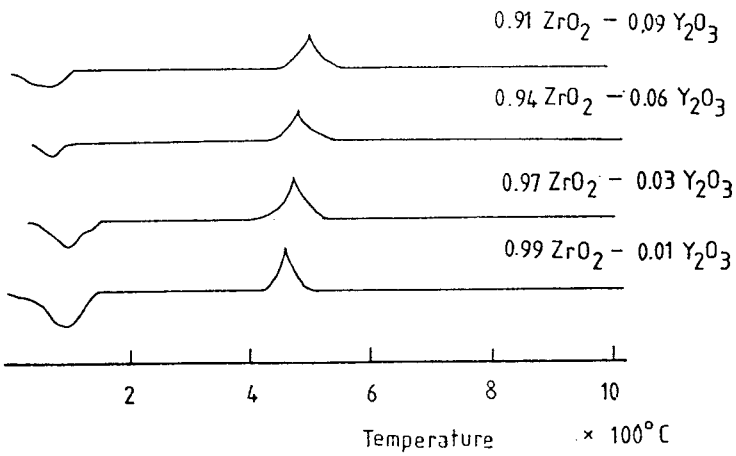

Fig. 14. DTA curves of powders prepared by spraying method in ZrO_2-Y_2O_3 system

3.2 ZrO_2-CaO system

3.2.1 Powder preparation

$Ca(OH)_2$ precipitates could not be obtained under pH13. In this case, $Ca(OH)_2$ might coprecipitate with $Zr(OH)_2$ as in ZrO_2-MgO system. But this system did not coprecipitate

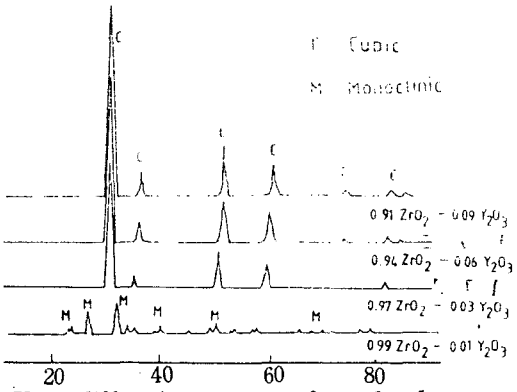

Fig. 15. X-ray diffraction patterns of powders heat-treated at 900°C

completely with NH_4OH. So in this experiment, $(NH_4)_2CO_3$ was used with NH_4OH to coprecipitate $Zr(OH)_2$ and $Ca(OH)_2$. The amount of $(NH_4)_2CO_3$ was 2 times of the mole of Ca. Raw materials in the Table 1 were used to prepare powders in $(1-x)ZrO_2$-xCaO system (x=0.05, 0.1,

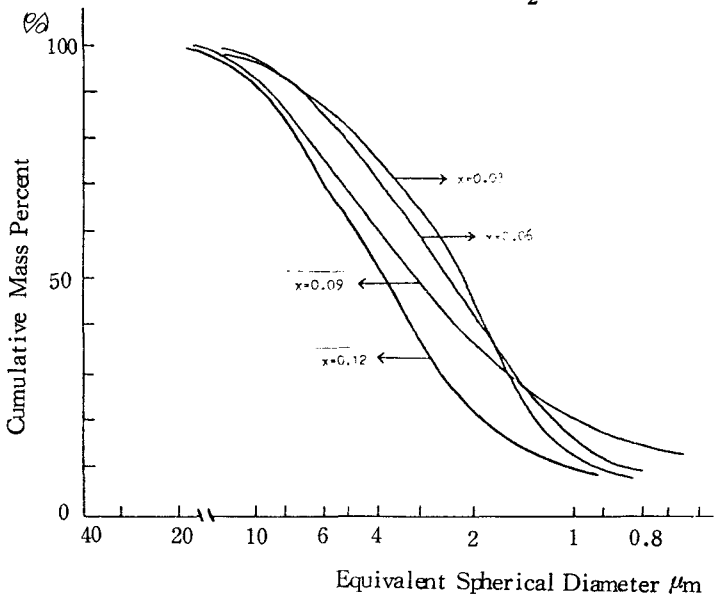

Fig. 16. Particle size distribution in ZrO_2-Y_2O_3 system

0.15, 0.2). Each solution was mixed in accordance with $(1-x)ZrO_2$-$xCaO$ for 12 hours on the magnetic stirrer. Mixed solution of raw materials was sprayed into the mixture of 5N-NH_4OH and $(NH_4)_2CO_3$ using apparatus of Fig. 3.

Table 3. Specific surface area of powders prepared by spraying method

Powder Composition	Specific Surface Area (m^2/g)
0.99 ZrO_2 - 0.01 Y_2O_3	250
0.97 ZrO_2 - 0.03 Y_2O_3	230
0.94 ZrO_2 - 0.06 Y_2O_3	290
0.91 ZrO_2 - 0.09 Y_2O_3	300

3.2.2 Characteristics of powder

Powders in this system had endothermic reactions at 100-200°C and exothermic reactions at 500-600°C. Crystallization temperature was shifted to the higher temperature with CaO content. These properties were same with **ZrO_2-MgO and ZrO_2-Y_2O_3 system (Fig.17)**.

X-ray diffraction patterns **(Fig.18)** of powders calcined at 900°C for 2hr showed cubic crystal phase.

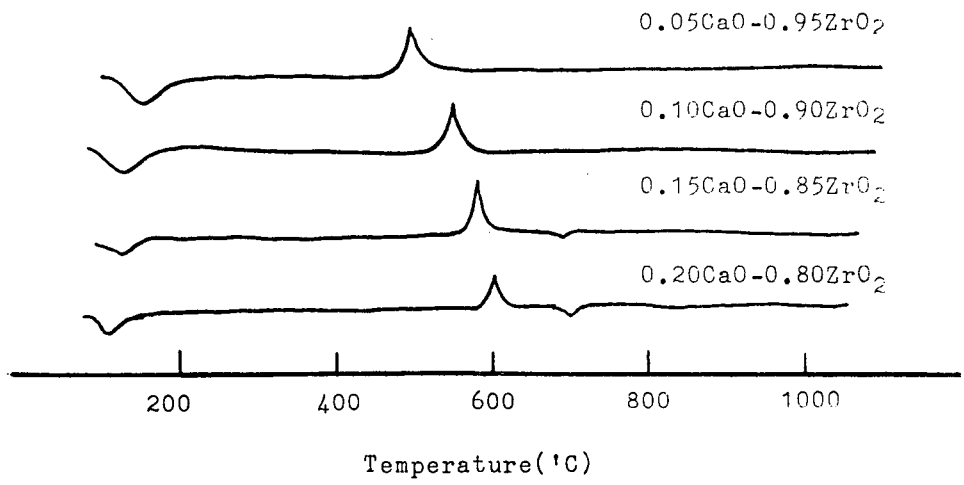

Fig. 17. DTA curves of samples prepared by spraying method in $(1-x)ZrO_2$-$xCaO$ system

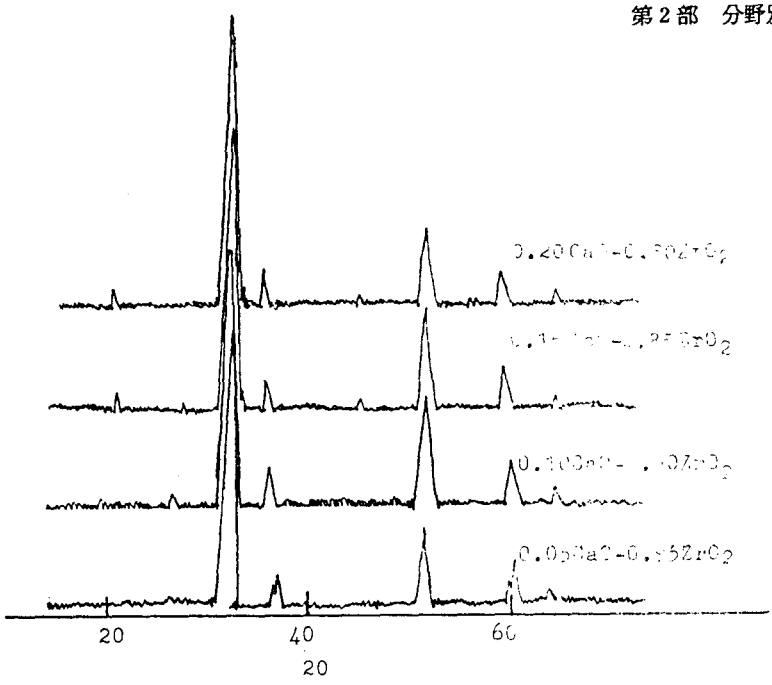

Fig. 18. X-ray diffraction patterns of powders heat-treated at 900°C

Scanning electronic micrographs (**Fig.20**) and particle size distribution (**Fig.19**) were sphere-shaped powders and narrow in the range 1-10μm as before.

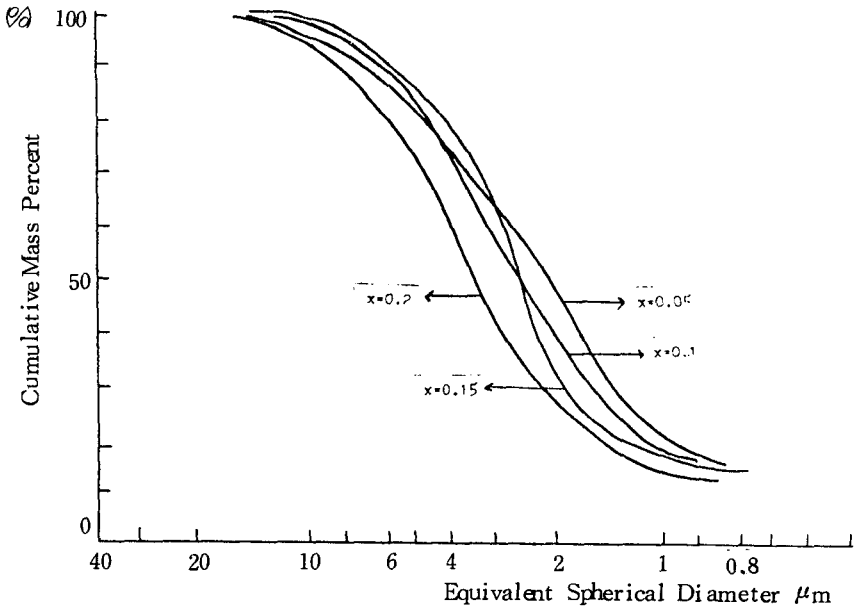

Fig. 19. Particle size distribution in ZrO_2-xCaO system

(a) x=0.05

10μm

(b) x=0.20

Fig. 20. Scanning electron micrographs of powders prepared by spraying method in ZrO_2- xCaO system

4. Ceramics in the system of ZrO_2-MgO, ZrO_2-Y_2O_3 and ZrO_2-CaO

4.1 Experimental procedure

Powders produced by spraying method were calcined at 900°C for 2hrs and cold-isostatic pressed into bar (0.4 X 0.4 X 3Cm) at 1.5ton/cm^2. The bar was put into electric furnace and heated to 1400°C, 1500°C and 1600°C for 2hrs. The heating rate was 5 °C/min. The specimens were furnace-cooled at a rate of 5°C/min to 1000°C. Further cooling to room temperature was somewhat slower.

Water absorption and density of the specimens fired at various temperature were measured. X-ray analysis of the surface of specimens fired at various temperature was done. The specimens were ground with SiC polishing paper (#400, #800, #1000, #1200) to measure 3-point MOR. Measuring conditions are as follows;

Load : 100Kg/F.S

Span Length : 20mm

Cross Head Speed : 4mm/min

Chart Speed : 5mm/min

Polished specimens with SiC polishing paper were ground finely by diamond paste of 6μm, 3μm and 1μm to remove damaged layer. Fracture toughness was determined at room temperature by using indentation technique. K value were calculated as below equation

$$K_{IC} = \frac{P}{\pi^{3/2} \cdot \tan\theta \cdot D^{3/2}}$$

where P : indentation load
D : crack length
θ : half angle of Vicker indenter ($\theta = 68°$)

4.2 Result and Discussion

4.2.1 ZrO_2 -MgO system

(a) water absorption and density

Fig.21 and **22** are the plot of water absorption percent and density. Water absorption decreased with increase of sintering temperature and MgO content. Densities were not increased so much with increasing sintering temperature but decreased with increase of MgO content because gravity of MgO is lighter than ZrO_2.

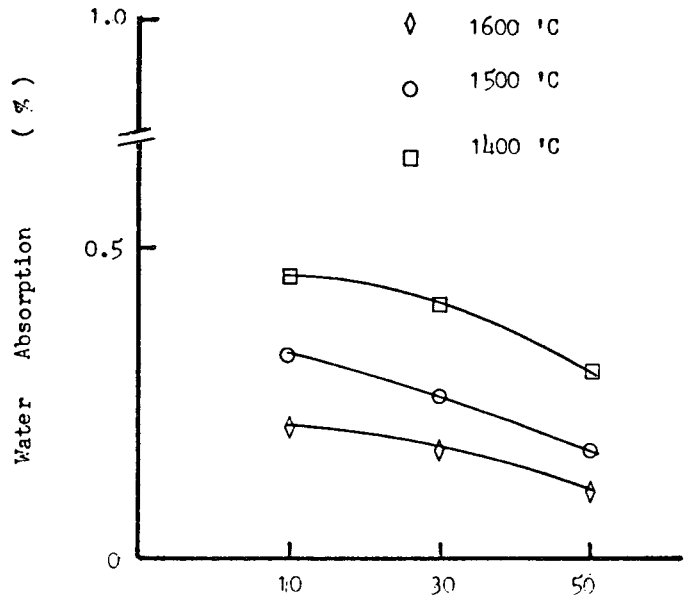

Fig. 21. Water absorption of samples with various MgO content

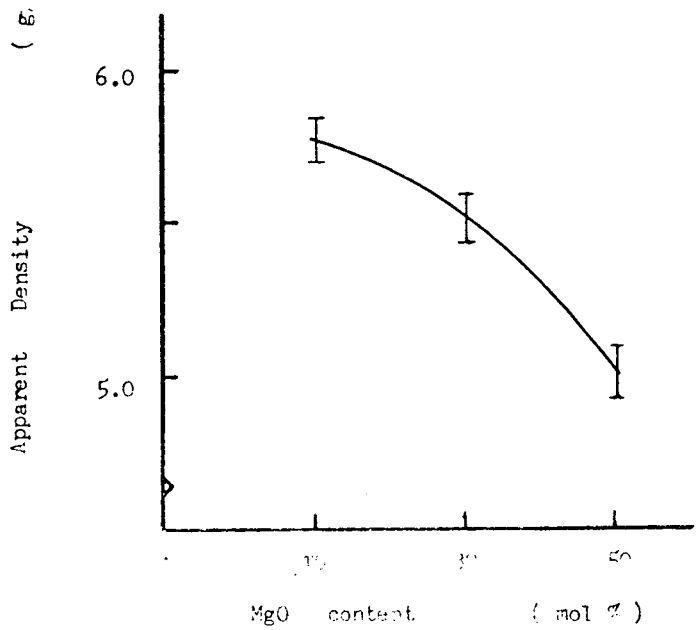

Fig. 22. Density of samples as a function of MgO content

(b) X-ray analysis

X-ray diffraction patterns of the specimens fired at 1500°C for 2hrs is **Fig.23** (same with 1400°C and 1600°C). Zirconia was stabilized above 30 mol% of MgO because crystal was only cubic phase. But at 10 mol% MgO, monoclinic cubic phases were coexisted in zirconia owing to transformation from metastable tetragonal to monoclinic at room temperature.[25,29]

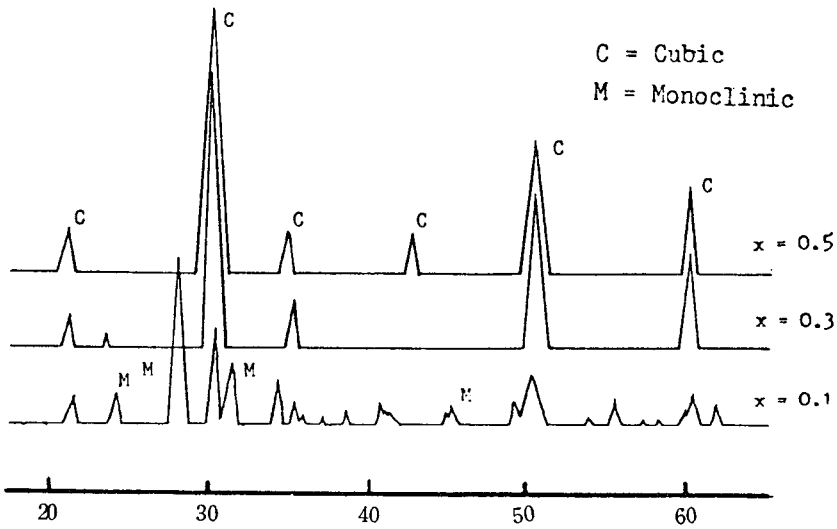

Fig. 23. X-ray diffraction patterns of specimens fired at 1500°C for 2hrs in (1-x) ZrO_2-xMgO system

(c) Strength and fracture toughness

The variation of the modulus of rupture of ground bar is shown in **Fig.24.** Strength was not changed so much with sintering temperature and MgO content and was 320 MPa on the whole.

The cirtical stress intensity factor, K_{IC}, as a function of firing temperature and MgO content is shown in **Fig.25**. This fracture toughness was not so different in sintering temperature but decreased with increasing MgO content. Zirconia with 10 mol% of MgO had the highest K_{IC} value, 15Kg/min$^{3/2}$. This property originated in martensitic transformation.[26,29,30]

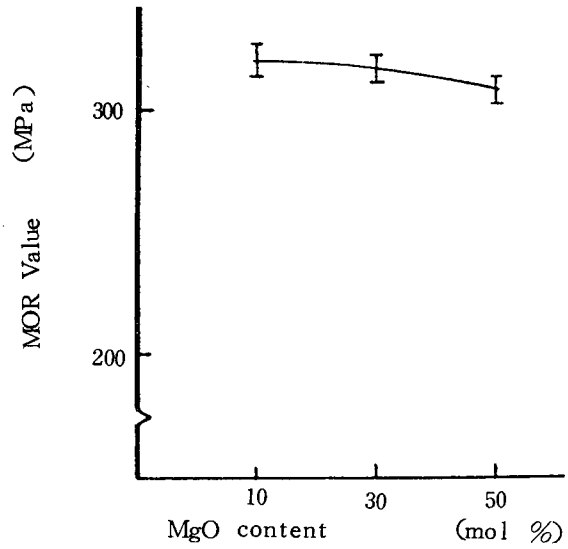

Fig. 24. 3-point MOR strength of samples with various MgO content

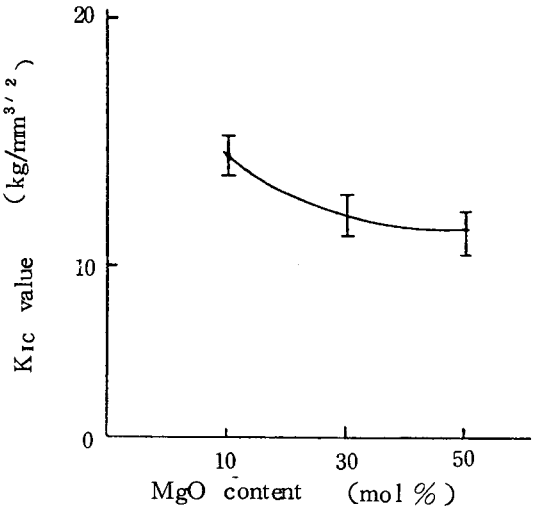

Fig. 25. Fracture toughness of samples (with MgO) fired at various temperature

4.2.2 ZrO_2-Y_2O_3 System

(a) Water absorption and density

Water absorption percent and density are shown in **Fig. 26** and **27** as a function of sintering temperature and Y_2O_3 content. Water absorption was minimum at 3 mol% of Y_2O_3 and decreased with increasing of sintering temperature. Density was maximum at 3 mol% of Y_2O_3

and increased with increasing of sintering temperature contrary to water absorption. Relative density showed 98% or more of theoretical density at 3 mol% of Y_2O_3 above 1500°C firing.

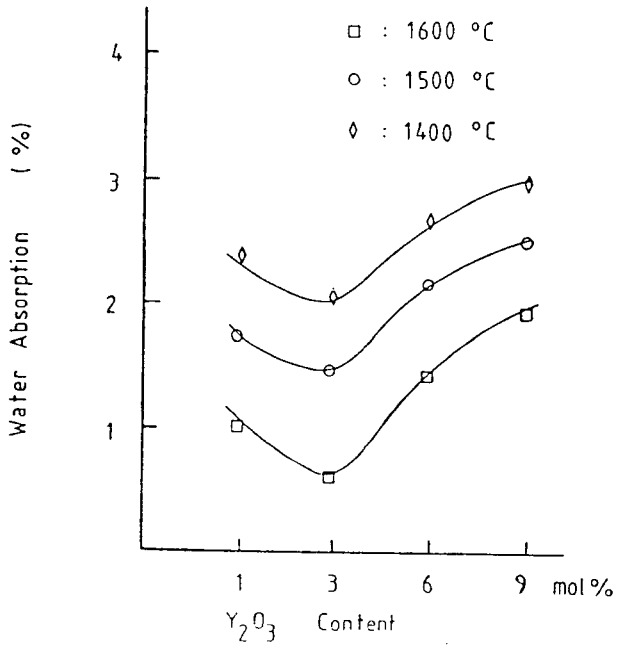

Fig. 26. Water absorption of specimens with various Y_2O_3 content

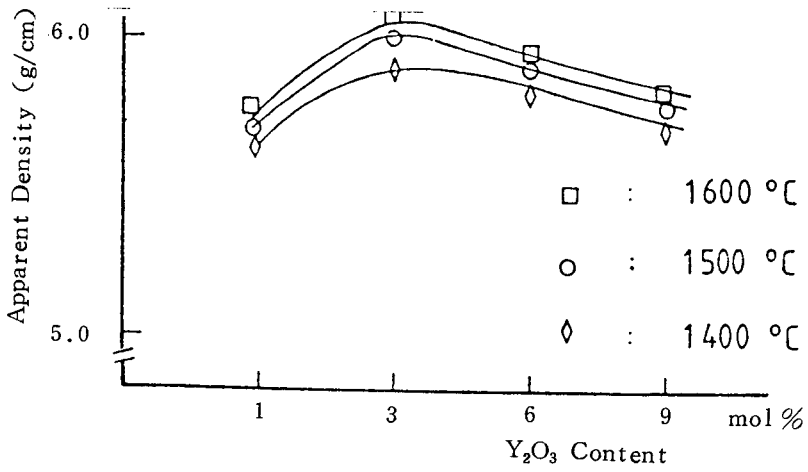

Fig. 27. Sintered densities of specimens with various Y_2O_3 content

(b) X-ray analysis

X-ray diffraction patterns of the specimens fired at 1500°C for 2hr is shown in **Fig. 28** (same with 1400°C and 1600°C). Zirconia was stabilized above 6 mol% of Y_2O_3 because crystal was only cubic phase. But at 3 mol% of Y_2O_3, monoclinic and cubic phase were coexisted in zirconia owing to transformation from metastable tetragonal to monoclinic at room temperature.[25,29]

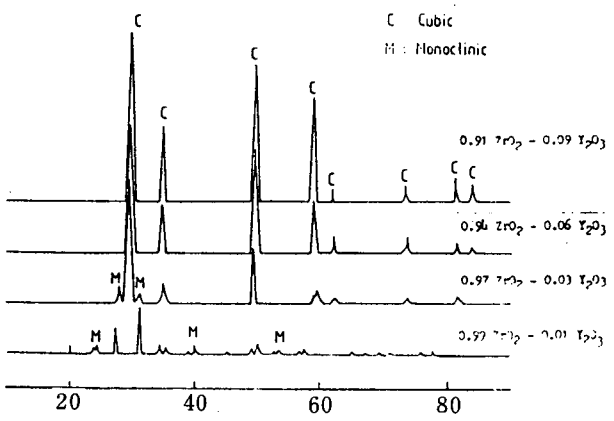

Fig. 28. X-ray diffraction patterns of specimens fired at 1500°C for 2hrs in ZrO_2-Y_2O_3 system

(c) Strength and fracture toughness

Fig.29 shows the variation of the modulus of rupture. At 1 mol% of Y_2O_3, the specimens

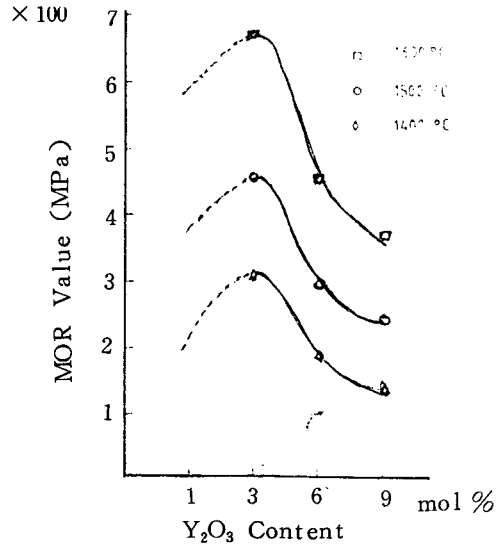

Fig. 29. 3-point MOR strength of specimens with various Y_2O_3 content

fired at various temperature were broken down because of volume change originated in phase transformation. The other specimens had tendency such as density and maximum MOR value, 700MPa was measured at 3 mol% of Y_2O_3.

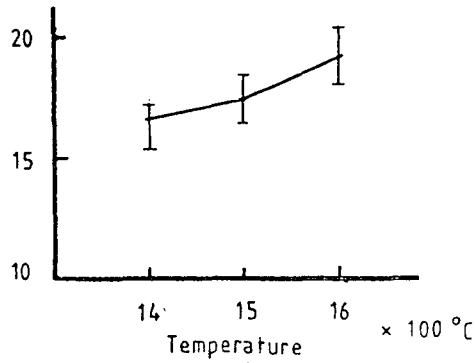

Fig. 30. Fracture toughness of specimens with 3 mol% Y_2O_3 fired at 1400°C-1600°C

The critical stress intensity factor, K_{IC} of zirconia with 3 mol% of Y_2O_3 is shown in **Fig.30** as a function of firing temperature. It was difficult to measure K_{IC} of the other specimen because they had considerable amounts of pore in the specimens. Zirconia fired at higher temperature had higher K_{IC} value. The specimen sintered at 1600°C had the highest K_{IC}, 19Kg/mm$^{3/2}$. This property originated in martensitic transformation.[26,29,30]

4.2.3 ZrO_2-CaO System

Fig.31 and **32** show the water absorption and density as a function of firing temperature and CaO content. Water absorption in this system was higher than any other system. Zirconia

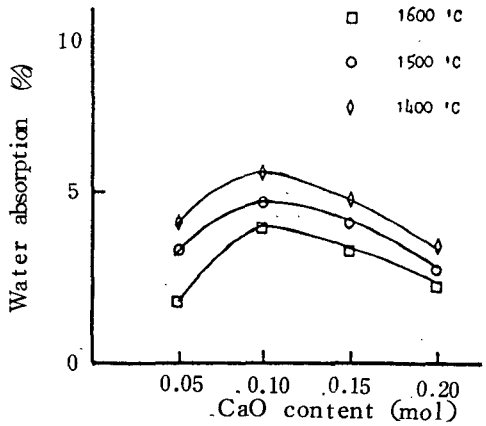

Fig. 31. Water absorption of specimens with various CaO content

with CaO was not sintered enough to characterize some properties in view of water absorption. Only X-ray analysis of specimens sintered at 1500°C is shown in Fig.33. Cubic phase only was above 15 mol% of CaO, and cubic and monoclinic phases were at 10 mol% of CaO.

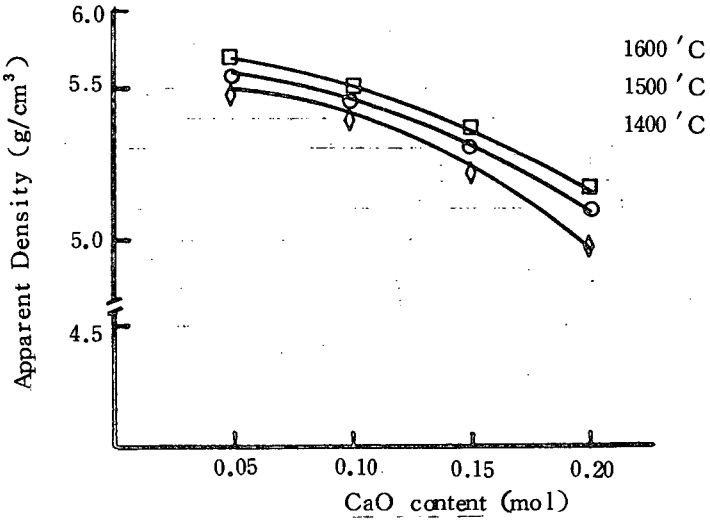

Fig. 32. Densities of specimens with various CaO content

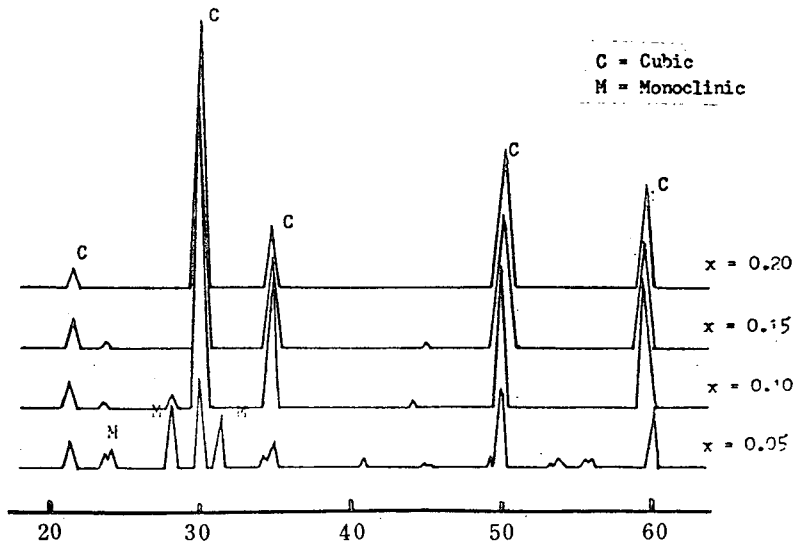

Fig. 33. X-ray diffraction patterns of specimens fired at 1500°C in ZrO2-CaO system

5. Conclusions

Powder preparation to reveal the specific functions were studied and the results were as follows.

1. Powders produced with spraying method had characteristics below
   a) Powder without agglomeration
   b) Sphere-shaped powders with diameter of 1-10μm
   c) Large surface area
   d) Spontaneous precipitation (not preferential precipitation)
   e) Mass production
2. Crystallization temperature was shifted to the higher temperature with increase of additives of MgO, Y_2O_3 and CaO
3. At 10 mol% of MgO, monoclinic and cubic phase were coexisted, but only cubic phase was above that in ZrO_2-MgO system.
4. At 3mol% of Y_2O_3, monoclinic and cubic phase were coexisted, but only cubic phase was above that in ZrO_2-Y_2O_3 system
5. Monoclinic and cubic phases were coexisted at 10 mol% of CaO, but only cubic phase was above that in ZrO_2-CaO system.
6. Zirconia with 10 mol% of MgO had the highest MOR, 320MPa and K_{IC}, 15Kg/mm$^{3/2}$.
7. Zirconia with 3 mol% Y_2O_3 had the highest MOR, 700MPa and K_{IC} 19Kg/mm$^{3/2}$.

Reference

1) Roger R. Wills and John Kelvin McCoy, "Interface-Reaction-Controlled Kinetics in the Hot Isostatic Pressing of Submicrometer Alumina Powder", J. Am. Ceram. Soc., 68(4) C95-C96 (1985)
2) Ivan B. Cutler and Roy E. Henrichsen, "Effect of particle shape on the kinetics of sintering of glass", J. Am. Ceram. Soc., 53(3) 136-141 (1970)
3) I. B. Cutler, "Active Powders", pp.21-29 in Ceramic Processing before Firing adited by G.Y. Onoda, Jr. and L. L. Hench (1978)
4) A. G. Pincus, "Realization of Fine-Grain Ceramics", pp.3-14 in Ultrafine-Grain Ceramics edited by J. H. Burke, N. L. Reed, and V. Weiss (1970)
5) F. F. Y. Wang, "Powder Characterization", pp.39-51 in Advances in Powder Technology edited by G. Y. Chin (1981)

6) R. Nathan Katz, "Characterization of Ceramic Powders", pp.35-49 in Ceramic Fabrication Process edited by F. F. Y. Wang (1976)

7) D. E. Niesz, R. B. Bennett, and M. J. Snyder, "Strength Characterization of Powder Aggregates", Am. Ceram. Soc. Bull., 51(9) 677-680 (1972)

8) Y. S. Kim, "Effect of Powder Characteristics", pp.51-70 in Ceramic Fabrication Process edited by F. F. Y. Wang (1976)

9) A. Roosen and A. Hausner, "Sintering Kinetics of ZrO_2 Powders", pp.714-726 in Advances in Ceramics vol. 12 edited by N. Claussen, M. Ruhle, and A. H. Heuer (1984)

10) S. Somiya, "preparation methods for zirconia fine powder" Zirconia Ceramics 1, pp.1-19 (1985)

11) M. Takahashi and S. Suzuki, "Deformability of Spherical Granules under Uniaxial Loading", Am. Ceram. Soc. Bull., 64(9) 1257-1261 (1985)

12) J. G. M. deLAU, "Precipation of Ceramic Powders From Sulfate Solutions by Spray Drying and Roasting", Am. Ceram. Soc. Bull., 49(6), 572-574 (1970)

13) R. E. Jaeger and T. J. Miller, "Precipation of Ceramic Oxide Powders by liquid drying", Am. Ceram. Soc. Bull., 53(12), 855-859 (1974)

14) M. Wuda, "Preparation of submicron metal and ceramic powders using plasmatic gas", Electronic ceramics July pp.15-21 (1985)

15) Suyama Y., T. Mizobe, and A. Kato, "ZrO_2 Powder Produced by Vapor Phase Reaction", Ceramuqia Int. 3(4) 141-146 (1977)

16) T.A. Wheat, "Preparation and Characterization of Lime-Stabilized Ziroconia", J. Am. Ceram. Soc., 42, 11 (1973)

17) Haberko. K. "Some Properties of Zirconia obtained by Coprecipitation with Different Oxides", Res. Int. Htes Temp. et Riefract +14, 217-224 (1977)

18) Y. Murase, E. Kato, and M. Hirano, "Preparation of Ultra-Fine Particles of Monoclinic ZrO_2 by Hydrolysis of $ZrOC_{12}$", Yogyo-Kyokai-Shi, 92(2) 18-24 (1984)

19) S. Sakka and K. Kamiya, "Preparation of Shaped Glasses through Sol-Gel method", Mater. Sci. Res., vol.17, 83-94 (1984)

20) K. S. Mazdiyasni, C. T. Lynch and J. S. Smith H., "Cubic Phase Stabilisation of Translacent Yttria-Zirconia at very Low Temperature", J. Am. Ceram. Soc., 50(10), 532-537 (1967)

21) P. Duwez, F. Odell and F. H. Brown, Jr. "Stabilization of Zirconia with Calcia and Magnesia", J. Am. Ceram. Soc., 35(5), 107-113 (1952)

22) R. F. Geller and P. J. Yavorsky, "Effect of Some Oxide Additives on Thermal - Length Changes of Zirconia", Ceram. Abstr., 24(10), 191 (1945)

23) F. H. McRitchie and N. N. Ault, "Design of a High Temperature Resistance Furnace", J. Am. Ceram. Soc., 33(1), 25-26 (1950)

24) D. Michel, "Relationship Between Morphology and Structure for Stabilized Zirconia Crystals", 17) Ibid.

25) G. K. Bansal and A. H. Heur, "Precipitation in Partially Stabilized Zirconia", J. Am. Ceram. Soc., 58(5-6), 235-238(1975)

26) F. F. Lange, "Transformation toughening", J. Mater. Sci., 17, 235-239 (1982)

27) M. Okumiya & K. Kuwabara, "Zirconia fusioncast refractories", Zrconia Ceramics 1, pp.181-189 (1983)

28) K. C. Radford, R. J. Bratton, "Zirconia electrolyte cells", J. Mater. Sci., 14, 66-69 (1979)

29) A. G. Evans and A. H. Heuer, "Riview-Transformation Toughening in Ceramics; Martensitic Transformations in Crack-Tip Stress Fields", J. Am. Ceram. Soc., 63(5-6), 241-248 (1980)

30) D. L. Porter, A. G. Evans, and A. H. Heuer, "Transformation-Toughening in Partially-Stabilized Zirconia (PSZ)", Acta Metallurgica, 27, 1649-1654 (1979)